Characterisation and analyses of museum objects using pXRF:
An application from the Delphi Museum, Greece

Ioannis LIRITZIS[1], Nikos ZACHARIAS[2], Ioulia PAPAGEORGIOU[3],
Anthoula TSAROUCHA[4], Eleni PALAMARA[2]

Abstract. *Twenty-six objects from the Delphi archaeological Museum, including nearby museum premises, have been analysed by portable XRF. The aim was their characterization, provenance and archaeological interpretations. Twenty-one miniature Corinthian ceramic vases, a bronze and a ceramic pyxis bearing powder, four pigments on ceramics and six elegant glass vases, were non-destructively measured in situ. The ceramic analysis seems to form one cluster with similar chemical traits. The clay is calcareous with relatively high iron and titanium contents. Slip painted surface was due to increased MgO and Fe_2O_3. Four elegant glass vases were statistically compared to about 270 published data of similar period for provenance study and investigating the mineral agents for colouring glass. In fact the clustering analysis forms one of the major analytical groups containing the Delphi samples and also samples from Rhodes and Satricum. Of the major findings is the highly toxic mercury as cinnabar (HgS), a red pigment very commonly used since antiquity, mixed with PbO white lead in face powders. Particular elemental variations in all groups are discussed. Multiple statistical analysis was used, such as, various hierarchical cluster versions, PCA, bi-plots. The case study provides a practical aid to archaeological interpretation and emphasizes the valuable use of portable XRF in museum studies on material culture ranging from various types and periods.*

Rezumat. *Un număr de 26 obiecte din patrimoniul Muzeului Arheologic din Delphi au fost analizate prin XRF portabil, în vederea caracterizării, stabilirii locului de proveniență și interpretării arheologice. 21 vase miniaturale corintice, un pyxis din ceramică și bronz conținând pulbere, patru pigmenți pe ceramică și șase vase elegante din sticlă au fost analizate in situ printr-o metodă non-destructivă. Patru vase elegante din sticlă au fost comparate cu 270 de obiecte similare datând din aceeași perioadă, investigându-se agenții minerali de colorare a sticlei. Acest studiu de caz constituie un element auxiliar practic acordat interpretării arheologice și pune în evidență valoarea folosirii XRF portabil în studiile muzeale asupra culturii materiale de diferite tipuri și datând din perioade diverse.*

Keywords: glass, ceramic, pyxis, powder, pXRF, glass, chemical elements, analysis, cluster.

[1] Laboratory of Archaeometry, Department of Mediterranean Studies, University of the Aegean, Rhodes. Corresponding author: liritzis@rhodes.aegean.gr.
[2] Laboratory of Archaeometry, Department of History, Archaeology and Cultural Resources Management, University of the Peloponnese, Kalamata.
[3] Department of Statistics, Economic University of Athens.
[4] Ephoreia of Antiquities of Phokis, Delphi, Phokis.

1. Introduction

The non-destructive capabilities of XRF are indeed particularly suited to research in art and archaeology, where the sample is unique, or its integrity has significant technical or aesthetic value. This is perhaps best exemplified in the examination of works of art, where the forensic aspects of the measurement may provide historical insight[5]. However, for each experimental situation, the choice of one approach over the other depends on the type and intrinsic value of the object, the aim of the investigation, the instruments available, and, last but not least, the scientist's or conservator's personal assessment of the acceptable damage.

Portable XRF (pXRF) analysers have shown during the last 30 years that they are ideal tools to aid in a variety of applications in cultural heritage, archaeology/geoarchaeology, and in archaeometry research in general[6], including:

a) On-site material characterization of lithic tools, ceramics. For example, ceramics for the examination of decorated shards, provenance of clay and trade[7];

b) Identification of mineral pigments in modern art[8] and binding media and varnishes used in medieval paintings and manuscripts[9];

c) Sediments from drilling boreholes based on the resulted quantitative data, distinguishing of the fluvial or the marine character of the successively deposited sediments in all studied cores became feasible[10];

d) In museum analysis pXRF can identify components of pigments in paintings and glazes, metal alloy content, provide the characterization of objects such as jewellery, silverware and weaponry, thereby assisting conservators in the preservation and restoration of artefacts, as well as aiding in constructing databases from analytical data for the scientific community;

e) Provenance studies based on the identified elements and their concentrations and by comparing sources and artefacts[11];

g) Glass[12]; eighteenth century Polish, Brandenburg and Saxon glassware[13], as well as EDXRF of Celtic glasses[14] and porcelain[15].

---

[5] LONGONI *et alii*, 1998; SPOTO *et alii* 2000.

[6] CESAREO *et alii* 1972; HALL *et alii* 1973; CESAREO *et alii*, 1996, 1999; LONGONI *et alii* 1998; LANGHOFF *et alii*, 1999.

[7] PAPAGEORGIOU & LIRITZIS 2007; PAPADOPOULOU *et alii*, 2007; JAVANSHAH ZEINAB 2018.

[8] VANDENABEELE *et alii* 2000a; LIRITZIS & POLYCHRONIADOU 2007.

[9] VANDENABEELE *et alii*, 2000b.

[10] ZACHARIAS *et alii* 2009.

[11] E.g, LIRITZIS & ZACHARIAS, 2010.

[12] ZACHARIAS *et alii*, 2008.

[13] KUNICKI-GOLDFINGER *et alii* 2000.

[14] WOBRAUSCHEK *et alii*, 2000.

[15] WU *et alii*, 2000.

In general, direct and *in situ* material characterization is a triggering task, and conclusive answers may come to light only with the use of a combination of calibrated portable sets that perform within an interdisciplinary environment of material scientists, museum object studies and geo-archaeologists.

Here we present a first non-destructive method of characterization employing the portable XRF devices for some characteristic archaeological objects from Delphi Museum: little votive vases from a sanctuary of archaic period, some extremely elegant glass vases and an unknown origin powder from a tomb of 5th c. BC.

The detected major, minor and trace elements are discussed from the characterization and technology/provenance point of view, in comparison to other similar objects and weigh the potential of these results in the frame of practical application, extraction of significant data and archaeological interpretation.

2. Materials and methods

The objects analysed in the present work correspond to a variety of different materials, including ceramics, glass, and powder contents of vessels. More specifically, the following objects were analysed:

1. Four glass vessels, used for storing perfume oils. They come from tombs of the 5th c. BC in Delphi. The glass vessels were made using the core technique, which originally appeared in Mycenaean times and reappeared at the end of the 7th–beginning of 6th c. BC. Three of the vessels have dark blue bodies with white and yellow zig-zag decorative patterns, whereas one (sample 1672) is opaque white. The variety of the shapes of the vessels (*amphoriskos*, *oinochoe* and *alabastron*) and their decoration demonstrate the inspiration and virtuosity of ancient glassmakers (Figure 1). One glass (inventory no 7871) from Delphi is not grouped with the remaining 3 glasses from Delphi. The remaining 3 glasses from Delphi (7870, 8802 and 7869) form a clear compact group: 1 clay perfume inv. 8742, 2 colourful blue glass perfume inv. 8802, 3 colourful glass perfume container, 4 alabastron, inv. 7872; 5 and 6 pointed amphorae inv. 7869 blue, inv. 7870 yellowish white.

2. Twenty miniature fine grained ceramic vases. Thousands of miniature votive vases found in the sanctuary of Kirra, miniature cups, *oinohoae* (wine vase), *kantharoi*, water jar, baskets, boxes, plates etc. The 6th–4th c. BC Corinthian *kotyliskes* or *skyfidia* are in fact part of the amount of terracotta dedications accumulated in a pit in front of the building attached to the temple of the sanctuary found at Kirra during excavations of the French Archaeological School of 1936 to 1938. The sanctuary seems to serve the needs of residents of Kirra and pilgrims of the Pan-Hellenic sanctuary of Delphi and tributes are dated from the late 6th c. BC

until the third quarter of the 4th c. BC[16]. Representative examples of the ceramic vases are shown in Figure 2.

3. In one ceramic cylindrical pyxis with lid a light pink fine powder (psimythio) was found in the interior and was analysed in order to identify the original content of the vessel (Figure 3). The object comes from the so-called tomb of "theater actress" excavated at Delphi and dated to 400–350 BC.[17]

Non-destructive X-Ray Fluorescence (p-XRF) analysis was applied on all artefacts and samples since the technique allows fast and in situ, non-invasive analytical characterization of archaeological material[18]. The set up used was a portable Bruker Tracer III SD, with a rhodium X-ray tube and Si-Pin diode detector. The beam diameter is approximately 3 mm[19]. The set-up is calibrated against metal alloys and clays with the use of standards and quantification is made using the S1PXRF software and based on FP routine[20]. For the glass objects, data quantification was made using S1PXRF software and a custom-built calibration curve, created in collaboration with the scientific personnel of Bruker; a detailed description of the calibration curve and the accuracy and precision achieved for the analysis of glass is provided elsewhere[21].

In order to optimise the analytical range, two settings were used for the analysis of the ceramics and glass samples: (1) an unfiltered low-energy excitation mode (high voltage set at 15 kV and current of 24 μA, analyses carried out under vacuum) was used for the analysis of major and minor elements (with an atomic number, Z, between 11 and 26 for ceramics and between 11 and 29 for glass); and (2) an Al/Ti filtered (0.012 inches Al plus 0.001 inches Ti) high-energy excitation mode (high voltage set at 40 kV and current of 12 μA) was used for the analysis of minor and trace elements with a high atomic number (Z>29 for ceramics, and Z>26 for glass). The collection time of each measurement was 120 sec. The samples were not cleaned prior to the analysis, however care was taken to select areas with no signs of past restoration treatment and free of corrosion products.

3. Glass analysis

The corrosion layers present on the samples, in addition to the well-known analytical limitations of XRF for the lighter elements, lead to a significant underestimation of the

[16] PARIENTE 1991.

[17] PERDRIZET 1908.

[18] LIRITZIS & ZACHARIAS 2010.

[19] MOROPOULOU *et alii* 2016.

[20] SOKARAS *et alii*, 2009.

[21] PALAMARA *et alii*, 2016.

Figure 1. Images of the glass vessels from Delphi, during the in situ XRF analysis

Figure 2. Representative examples
of the miniature ceramic vases found at Kirra

Figure 3. Image of the ceramic vessel
with its content (pink powder)

Table 1. XRF compositional analysis of the glass vessels (major oxides in weight %, minor elements in ppm, normalised to 100%, "nd": not detected). A mean Na_2O (20.4 wt %) and MgO value (0.7 wt%) was estimated based on bibliographic data

Sample	Na_2O	MgO	Al_2O_3	SiO_2	SO_3	K_2O	CaO	Fe_2O_3	P	Ti	Mn	Co	Cu
1672	20.4	0.7	3.33	67.62	0.81	0.17	6.23	0.74	498	nd	188	nd	nd
1673	20.4	0.7	2.38	70.39	0.54	0.27	5.32	nd	28	nd	143	642	330
1674	20.4	0.7	3.80	67.43	1.01	0.29	6.20	0.16	375	33	167	389	257
1675	20.4	0.7	3.08	65.02	1.56	0.49	7.49	1.26	524	260	159	137	302

sodium content. To overcome this problem, Zacharias *et alii* (2008) suggest the replacement of the sodium and magnesium value by a value calculated by a different technique, or by using an estimate value from published data of similar glasses with those under study. The remaining percentage is then distributed to all remaining components on the basis of their relative XRF values. A mean value of the Na_2O and MgO concentration (20.4 and 0.7 wt%, respectively) was estimated based on the composition of contemporary and stylistically similar core-formed glass vessels from Thebes[22]. The XRF values that occurred for the major and minor elements of each sample, after re-normalizing to 100%wt, are presented in Table 1. It must be noted that the calibration curve of the trace elements is currently underway; therefore the available data correspond only to the light and mid-range elements of glass.

The data of the four Delphi vessels were compared against bibliographic data from contemporary sites in the Mediterranean region. Figure 4 presents Al_2O_3 versus CaO concentrations for the samples of the present assemblage along with recently published data from the following assemblages, in an effort to characterize its base glass. The published data consist by:

– 70 samples, primarily beads, from Rhodes, Greece. The samples date to approximately 640–600 BC[23];

– 29 glass beads from Thebes, Greece. The majority of the samples date to the archaic period (6th c. BC), but a few classical and Hellenistic samples (5th–3rd c. BC) are also present[24];

– 8 core-formed vessel fragments from Thebes, Greece. The samples date to the classical period (5th–4th c. BC)[25];

– 56 samples from Satricum, Italy, including 53 fragments of core-formed vessels and three fragments of beads. The samples date to the 4th–3rd c. BC[26];

---

[22] OIKONOMOU *et alii* 2012.

[23] OIKONOMOU *et alii* 2012.

[24] OIKONOMOU *et alii* 2012.

[25] ZACHARIAS *et alii* 2012.

[26] OIKONOMOU *et alii* 2016.

– 16 core-formed vessel fragments from the Pichvnari necropolis in Georgia. The samples date to the 5th c. BC[27];

– 59 vessel fragments or primarily monochrome bowls from Jebel Khalid, Syria. The samples date between the late 2nd and early 1st c. BC[28];

– 30 objects, including beads, jars and gaming pieces, from Pydna amd Methoni, Pieria municipality, Greece. The samples date between the 8th and 4th c. BC[29].

According to this biplot the samples from Rhodes have distinctively lower alumina concentration compared to all other assemblages. The samples from Thebes show a wide distribution; however, a subset of the Theban samples, demonstrating high alumina and relatively low calcium concentration[30], shares similar chemical traits with the four samples from Delphi, suggesting a similar technological tradition.
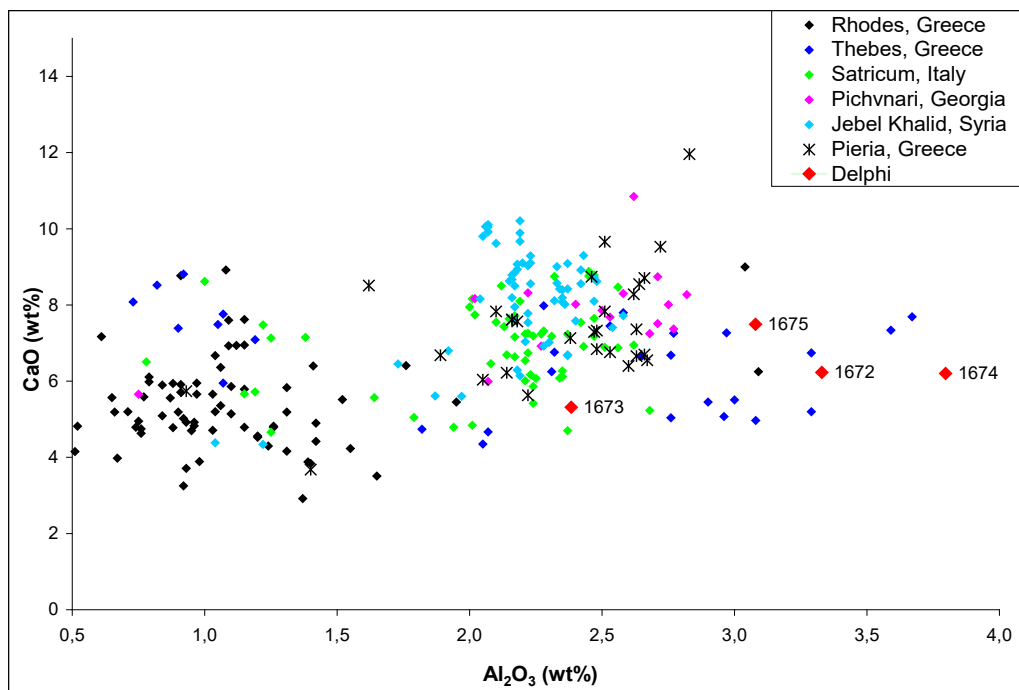

Figure 4. Al_2O_3 versus CaO concentrations for the glass samples of Delphi along with published data from Rhodes and Thebes, Greece (Oikonomou *et alii* 2012), Satricum, Italy (Oikonomou *et alii* 2016), Pichvnari, Georgia (Shortland & Schroeder 2009), Jebel Khalid, Syria (Reade & Privat 2016) and Pieria, Greece (Blomme *et alii* 2017)

[27] SHORTLAND & SCHROEDER 2009.

[28] READE & PRIVAT 2016.

[29] BLOMME *et alii* 2017.

[30] BELTSIOS *et alii*, 2012.

The same samples were further examined using Cluster Analysis based on all major oxides (with the exception of Na$_2$O and MgO, the values of which were not measured with satisfactory accuracy for the four samples from Delphi). The scope of the analysis is to reveal any relation of the four under study samples from Delphi with samples from the broad area of Mediterranean region. The clustering methods used for the analysis include hierarchical cluster analysis[31], and model-based cluster analysis[32] a framework which allows statistical testing for the number of existing groups in data. Various transformations of the data variables have been explored and principal component analysis (PCA) is used for plotting the results and evaluating the results of grouping.

Removing some clear outliers from the data set of total 285 observations, three main groups are initially formed. Figure 5 is a graphical representation of the resulting grouping on the first three PCs. One group consists of the observations from Rhodes, a second group labelled as group B with the distinctive feature of high value of Fe and group A which consists of all remaining, at this stage, observations. One of the four samples from Delphi, namely sample with label '1675' belongs to group B with high value of Fe. However, taking into consideration the fact that the results correspond to surface analyses on corroded samples, the observed differences of sample 1675 are most probably related to analytical problems, and not to the use of different raw materials. Figure 6, is plotted using the labels of the four samples from Delphi to gain information about their relative position.

At the next stage of the cluster analysis, focus is made in the majority of samples, labelled as group A, since the two other groups are distinctly different. Four groups are formed within group A and Figure 7 shows the resulting grouping in the first two principal components. The result is attained using model based cluster and the best model with respect to covariance matrices of the groups was the diagonal with varying volume and shape. The software used in 'mclust' package in R. Group 1 exhibits a wide spread and consists mainly of samples from Thebes and a subgroup of Satricum. The remaining three samples from Delphi belong to this group. Group 2 consists of samples from Syria and group 3 and 4 correspond to samples from Satricum, Italy. Appendix A (at the end) provides each group in detail. Figure 7/b shows the position of the three under study samples from Delphi with respect to the resulting groups.

In total, based on the above statistical approach, the Delphi samples belong to one of the major analytical groups containing the Delphi samples and also samples from Rhodes and Satricum.

---

[31] See for example EVERITT *et alii*, 2011.

[32] See BANFIELD & RAFTERY 1993.

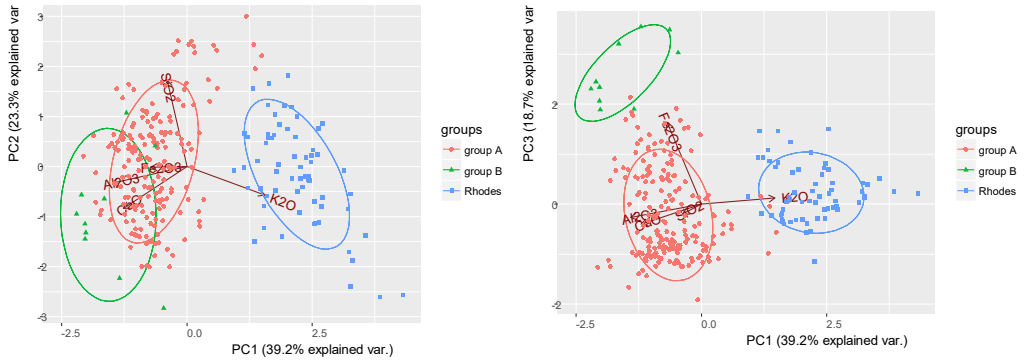Figure 5. Clustering result using the first three PCs. The number in parenthesis in label axes is the proportion of the total variability that each component explains
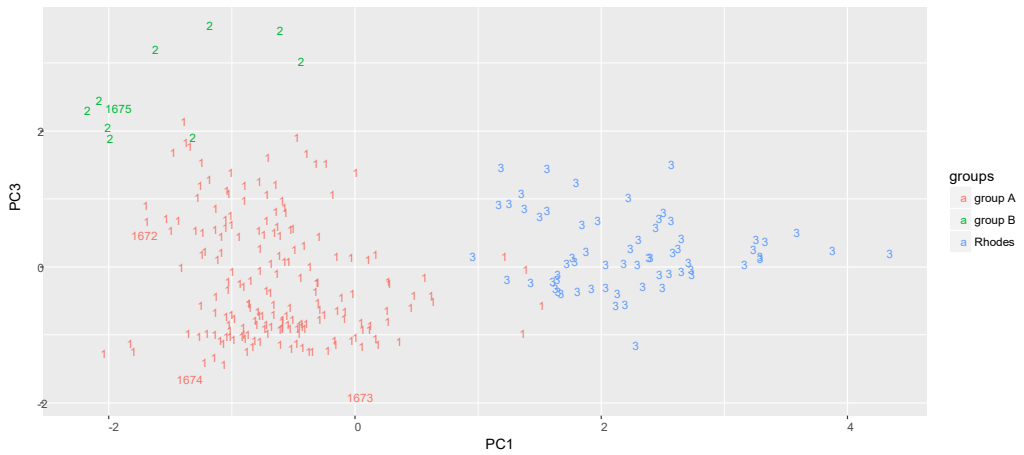

Figure 6. The clustering result on the first and third PCs using as labels the cluster membership with exception. The actual label names have been used for the four samples from Delphi
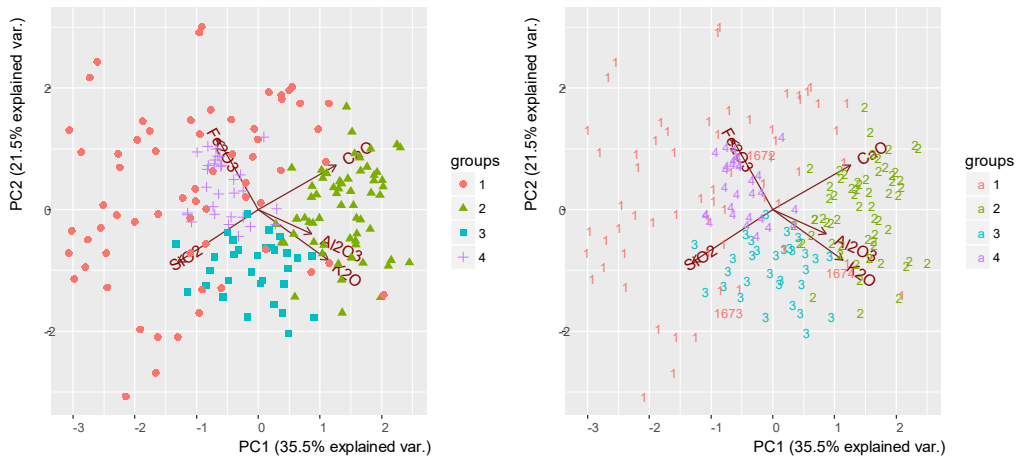

Figure 7. Cluster Analysis result presented in PCA components

4. Ceramics analysis

The analysis targeted to characterize the clay surface of the assemblage aiming towards the technological fingerprinting of their production technology. The chemical composition of the major and trace elements of the ceramic vessels are presented in Tables 2 and 3 respectively. Based on the major elements, the vast majority of the samples seem to form one cluster with similar chemical traits (Figure 8). The clay is calcareous with relatively high iron and titanium contents. The increased MgO and Fe_2O_3 values of samples 27023 and 27037 should be attributed to the accidental presence of slip within the area of analysis, and not to a chemically diverse fabric. The observed differences are likely associated with a coarser fabric; however, based on the major oxides, all samples seem to originate from the same clay source (Figure 8). The only sample which demonstrates different composition is sample 26835, which is characterised by high calcium and iron contents.

Table 2. XRF compositional analysis of the major oxides of the ceramic vessels (in weight%, normalised to 100%)

Sample	Na_2O	MgO	Al_2O_3	SiO_2	SO_3	K_2O	CaO	TiO_2	MnO	Fe_2O_3
26835	1.94	1.47	8.04	35.38	1.66	3.05	23.91	1.90	0.19	22.47
26850	1.56	1.44	11.04	40.26	3.67	0.99	19.94	1.12	0.08	19.89
27007	1.49	1.02	14.80	41.89	0.30	2.99	17.01	1.42	0.14	18.95
27008	1.05	1.35	14.52	47.05	2.86	1.12	17.64	1.15	0.08	13.18
27023	1.33	7.66	6.56	38.40	0.67	1.19	15.64	1.25	0.11	27.19
27024	1.55	1.05	9.74	40.65	5.38	1.70	18.66	1.32	0.09	19.85
27025	1.39	0.70	13.28	42.40	3.51	1.86	18.61	1.29	0.08	16.87
27035	0.91	1.86	15.96	48.96	1.50	1.57	16.24	1.05	0.08	11.88
27036	1.23	0.72	16.53	47.08	0.28	2.13	16.34	1.09	0.08	14.54
27037	1.55	3.80	8.86	40.76	0.59	2.39	13.70	1.46	0.10	26.78
27039	1.42	0.79	14.07	41.82	3.04	1.93	18.28	1.13	0.09	17.43
27040	1.46	1.10	13.37	45.43	1.21	2.08	15.20	1.28	0.10	18.76
27041	1.48	1.81	11.47	52.19	0.46	2.80	10.05	1.50	0.11	18.13
27044	1.37	1.08	13.34	47.78	2.34	1.96	13.16	1.28	0.08	17.60
27050	1.53	1.23	10.30	42.64	3.55	1.80	18.62	1.40	0.10	18.83
27082	1.34	1.02	13.69	51.26	1.03	2.47	11.71	1.35	0.10	16.03
27085	1.34	0.72	14.33	47.88	1.16	2.26	14.81	1.45	0.10	15.94
27089	1.49	2.07	10.68	45.57	3.37	1.89	15.07	1.37	0.08	18.42
8495	1.25	0.89	12.98	45.73	2.50	1.23	19.88	1.30	0.10	14.16
8497	1.19	0.82	14.85	46.14	1.06	1.87	18.13	1.15	0.11	14.68

Cluster Analysis, both hierarchical and model-based, was further undertaken for the 20 ceramic samples, using the values of both major and trace elements: Na_2O, MgO, Al_2O_3, K_2O, CaO, TiO_2, Ti (in ppm), MnO, Fe_2O_3, Cr, Co, Ni, Cu, Zn, Pb, Rb, Sr, and Zr.

All different clustering methods and various linkages within the hierarchical cluster analysis suggest that sample 26835 is different compared to others. The same result is confirmed with various data transformations, such as standardization. Figure 9 is a representation of the data in the first two principal components which account for the 51% of the total variation of the data. The variables with high impact in the first principal component are Na_2O, Al_2O_3, K_2O, TiO_2, Ti (in ppm), MnO, Fe_2O_3, Cu, and Sr.

Table 3. XRF compositional analysis of the minor and trace elements (in ppm, "nd": not detected)

| Sample	P	Ba	V	Cr	Co	Ni	Cu	Zn	As	Pb	Th	Rb	U	Sr	Y	Zr	Nb	Mo	Sn	Sb
26835	nd	1023	109	110	32	195	510	nd	16	17	8	76	nd	269	24	97	7	16	4	49
26850	nd	169	nd	96	31	224	256	11	35	22	9	90	nd	481	27	96	8	nd	3	22
27007	nd	864	32	93	33	239	147	112	13	16	8	88	3	366	25	119	9	nd	3	22
27008	176	1769	11	105	33	248	162	115	15	16	9	99	nd	375	29	112	9	nd	3	14
27023	nd	nd	nd	61	30	226	119	74	12	17	8	82	1	348	26	120	9	2	3	25
27024	nd	833	5	94	34	280	126	70	11	16	9	85	nd	272	27	124	9	nd	3	20
27025	105	865	7	101	33	246	258	25	23	20	9	94	3	334	26	112	9	nd	3	20
27035	347	1646	9	111	32	264	142	64	23	20	10	103	2	410	27	119	10	nd	3	14
27036	125	716	17	104	30	230	144	55	10	16	9	104	2	380	27	115	10	nd	3	20
27037	nd	nd	nd	84	38	280	257	97	37	22	10	116	3	262	26	121	10	nd	3	24
27039	38	848	nd	94	34	263	135	111	77	29	10	80	nd	413	33	111	9	nd	3	17
27040	nd	522	7	95	36	276	146	79	59	26	10	96	nd	336	31	116	9	nd	3	14
27041	nd	575	nd	73	28	197	102	124	34	22	11	121	1	319	27	125	11	2	3	28
27044	nd	581	nd	84	32	201	137	81	20	19	10	111	7	397	25	122	11	nd	3	22
27050	nd	877	14	86	34	250	139	89	18	18	10	115	7	335	24	118	11	nd	3	19
27082	nd	528	3	113	32	257	279	44	147	36	11	100	1	299	28	115	9	nd	3	19
27085	nd	863	28	96	31	194	119	103	12	16	11	123	nd	305	27	122	10	nd	3	18
27089	nd	126	nd	82	29	170	200	63	24	20	11	115	2	338	27	129	10	nd	3	18
8495	379	1607	38	92	28	183	197	294	627	63	12	81	nd	343	27	93	8	10	4	34
8497	nd	1836	28	92	34	244	140	205	29	20	10	114	9	446	22	114	10	nd	3	22
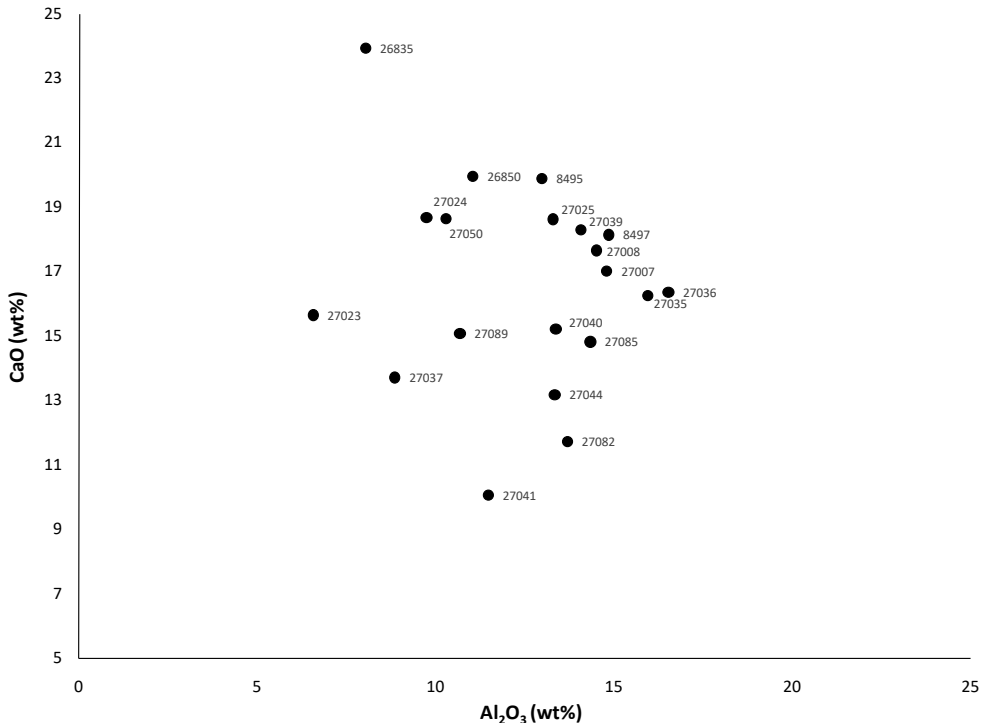
Figure 8. Al$_2$O$_3$ versus CaO concentrations for the ceramic samples of Delphi
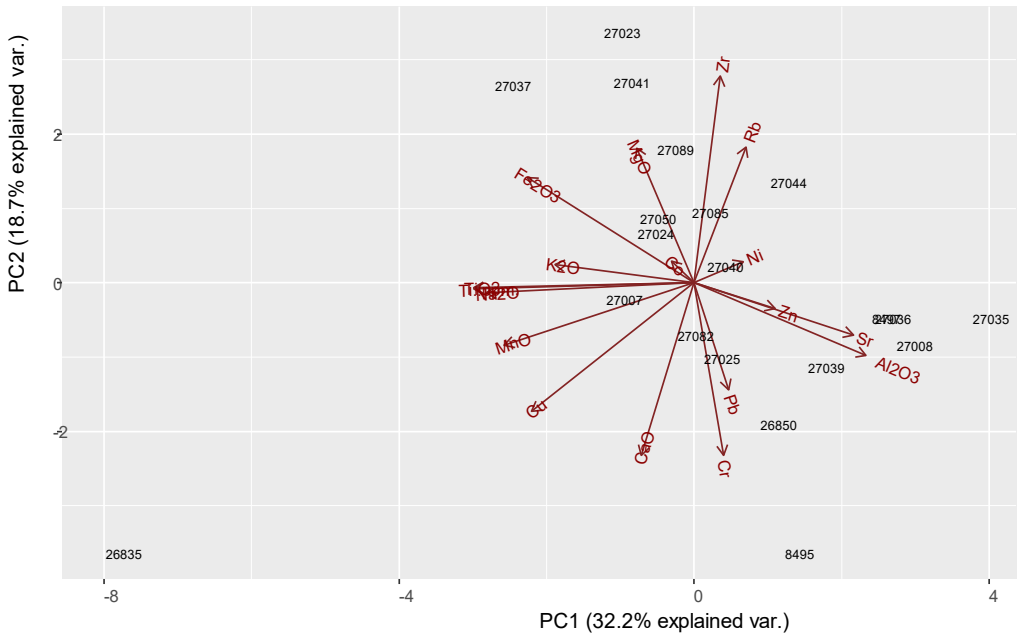

Figure 9. Biplot of Principal Component Analysis on Standardized data

Removing sample 26835 and after repeating the procedure two subgroups are more apparent. Figure 10 shows the dendrograms of the remaining data when complete and average linkage techniques, the two most widely used linkages in hierarchical clustering, are implemented. Analytically, the two sub-groups, noted as 1 and 2 respectively, consist of the samples:

Group 1	27023 27008 27035 8497 26850 8495 27025 27039
Group 2	27099 27024 27050 27044 27082 27085 27007 27037 27041

Figure 11 is the biplot of the principal component analysis with the data points to be labelled according to their group membership. Conclusions drawn from the biplot are that group 1 to the right side of the graph contains samples which are mainly characterized from their high value of Al_2O_3, Cr, Sr, CaO, Pb, Cu, and Ni and small value to all remaining elements. The exact opposite situation holds for samples in group 2. They indicate low measurement values in those elements and high to all remaining. A small exception may be noted for sample 27023, which exhibits the same profile with samples in group 1 with a higher value, relative to the remaining group, in MnO.

Overall, the ceramic samples under study show similar chemical fingerprinting and within the observed, relative, homogeneity two subgroups can be seen reflecting the possibility of either the existence of two different workshops or of differentiating production series, operating within the same geographical area.

5. Powders analysis

a) The XRF analysis of the pink powder, found in one of the ceramic vessels lead to the determination of the original content. This powder from a ceramic pyxis originates from tomb AMΔ 4321. It is a clay cylindrical pyxis with lid and it retains its light pink powder content (psimythio). It comes from the so-called tomb of a "theatre actress" excavated at Delphi and dated in 400–350 BC[33]. The identification of Sulphur (S) and Mercury (Hg) but Pb as well clearly identifies the powder as cinnabar, that is HgS a red pigment very commonly used since antiquity, mixed with PbO white lead (Figure 12). The 4th c. BC Greek author Theophrastus mentioned three different sources of cinnabar: from Spain, from Colchis in present-day Georgia, and in Ephesus in Asia Minor[34]. The parallel presence of lead (Pb) can either be attributed to impurities in the cinnabar ore or to the mixing of a lead-based pigment with cinnabar[35]. The most striking property of cinnabar is its red colour. Its bright colour

---

[33] PERDRIZET 1908.

[34] EASTAUGH *et alii* 2004.

[35] NÖLLER 2015.

makes it easy to spot in the field and is a fascination for those who discover it. It has a Mohs hardness of 2 to 2.5 and is very easily ground into a very fine powder. It has a specific gravity of 8.1, which is extremely high for a nonmetallic mineral. Cinnabar has also been used in powdered form for ritual blessings and burials. Powdered cinnabar was used as a cosmetic in many parts of the world for thousands of years. Eventually it was discovered that cinnabar is
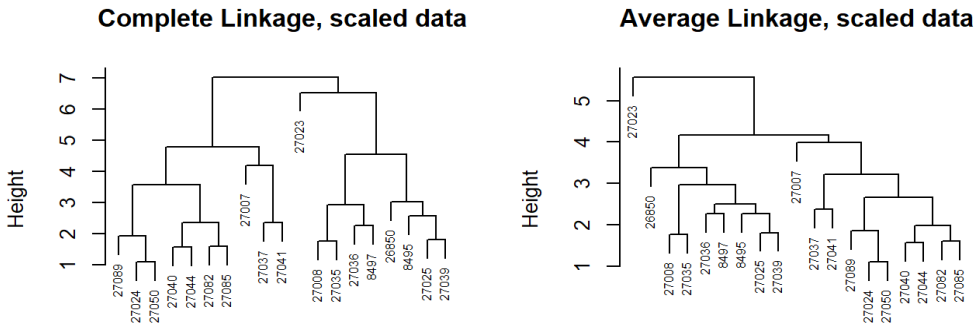

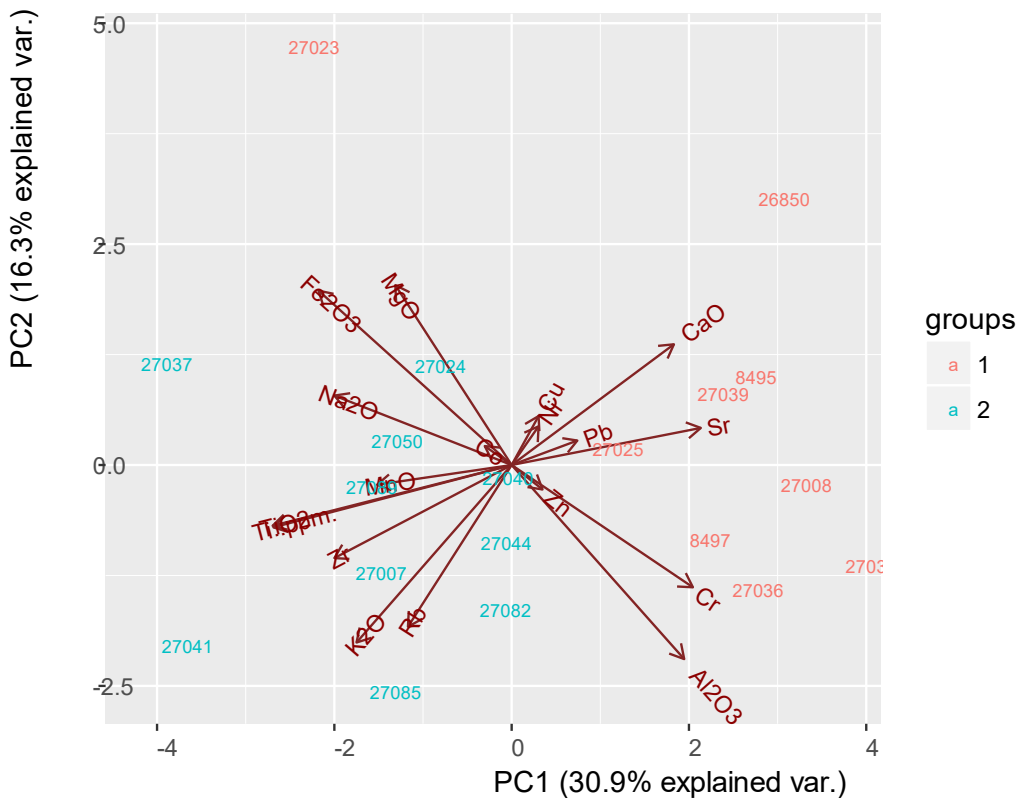Figure 10. Hierarchical cluster analysis with average and Ward linkage methods

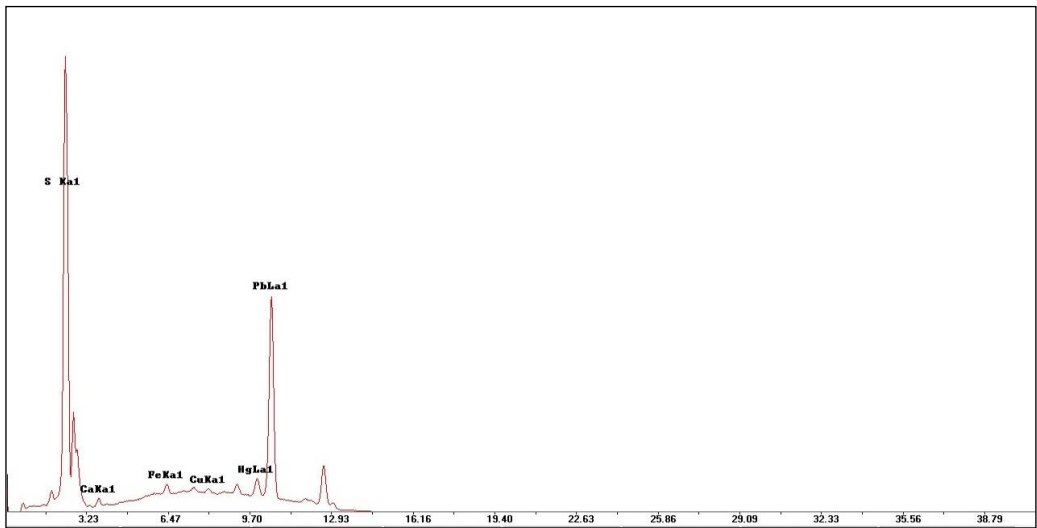Figure 11. The cluster analysis result plotted in biplot of PCA

Figure 12. Representative XRF spectrum of the pink powder
found inside a ceramic vessel showing Hg, Pb, S, Ca, Fe

Figure 13. Bronze cylindrical compass with lid and powder inside

toxic, and its use in pigments, paints, and cosmetics began to decline. In oil paintings, Pierre Renoir (1919) often used cinnabar mixed with lead white to create a rose coloration, mainly for skin. Together with calcined crystal glass (30% Pb), this coloration is very stable. Leonardo da Vinci (1519) mixed 99% lead white with 1% HgS to create a special brightness in the brownish layers of Mona Lisa's face[36]. It is striking the use of face colouring in the Middle Ages, after almost 2000 years since its use in ancient Greece. Inhalation from vapours of dust causes health problems in lungs and nervous system.

b) The Bronze cylindrical compass AMA 3692 with lid was derived from a cist grave that was discovered in 2001 about two kilometres off the Amfissa, in the opening work of the road[37] (Figure 13). This metal find (3692) was found to be bronze (*oreichalcus*) Cu-Zn (81.8%-14.6%) with some Pb (1.06%) and Sn (1.68%). Powder within this metal vase was Cu with lower content in Zn, Ca and Fe, indicating corrosion.

All above analysis and discussion per se help archaeological interpretation and conservation purposes employing a portable non-evasive and quite accurate technique compared to other desktop instrumentation[38].

6. Conclusion

The use of non-destructive XRF on Museum materials in Delphi has given important information regarding manufacturing, characterization and provenance of production. Glass, ceramic vases, powders and metal by products are analysed and robust statistical techniques were applied. Differentiating between clay or glass or powder was based on detailed statistical clustering and biplots, and the results were useful to archaeologists in Delphi Museum.

References

ABDEL RAHIM, N.S. 2016a. Roman coloured glass objects excavated from Tripoli, Libya: A chemico-physical characterization study. *Middle East Journal of Applied Sciences* 6(3), 594–605.

ABDEL RAHIM, N.S. 2016b. Analytical study and conservation of archaeological terra sigillata ware from Roman period, Tripoli, Libya. *Scientific Culture* 2(2), 19–27.

BANFIELD, J.D., A.E. RAFTERY 1993. Model-based Gaussian and non-Gaussian clustering. *Biometrics*, 49: 803–821.

---

[36] ELIAS & COTTE 2008.

[37] KOLONIA & TSAROUCHA, 2004.

[38] See ABDEL RAHIM 2016a; 2016b; CAKAJ *et alii*, 2016.

BELTSIOS, K.G., A. OIKONOMOU, N. ZACHARIAS, P. TRIANTAFYLLIDIS 2012. Chapter 13. Characterisation and provenance of archaeological glass artifacts from mainland and Aegean Greece. In: I. Liritzis I., C. Stevenson (eds) *The dating and provenance of volcanic and ancient manufactured glasses-a global overview*, 166–184. Albuquerque.

BLOMME, A., P. DEGRYSE, E. DOTSIKA, D. IGNATIADOU, A. LONGINELLI, A. SILVESTRI 2017. Provenance of polychrome and colourless 8th–4th c. BC glass from Pieria, Greece: A chemical and isotopic approach. *Journal of Archaeological Science* 7, 134–146.

ÇAKAJ, O., T. DILO, G. SCHMIDT, N. CIVICI, F. STAMATI 2016. Fibula and snake bracelet from Albania. A case study by OM, SEM/EDS and XRF. *Scientific Culture* 2(2), 9–18.

CESAREO, R., F.V. FRAZZOLI, C. MANCINI, S. SCIUTI, M. MARABELLI, P. MORA, P. ROTONDI, G. URBANI 1972. Non-destructive analysis of chemical elements in paintings and enamels. *Archaeometry*, 14(1), 65–78.

CESAREO, R., GIGANTE, G.E., CANEGALLO, P., CASTELLANO, A., IWANCZYK, J.S. AND DABROWSKIE, A. 1996. Applications of non-cryogenic portable EDXRF systems in Archaeometry. *Nuclear instruments and methods in Physics research Section A: Accelerators, spectrometers, detectors and associated equipment,* 380(1–2), 440–445.

CESAREO, R., G.E. GIGANTE, A. CASTELLANO 1999. Thermoelectrically cooled semiconductor detectors for non-destructive analysis of works of art by means of energy dispersive X-ray fluorescence. *Nuclear instruments and methods in Physics research Section A: Accelerators, spectrometers, detectors and associated equipment* 428(1), 171–181.

EASTAUGH, N., V. WALSH, T. CHAPLIN, R. SIDDALL R. 2004. *The pigment compendium. A dictionary of historical pigments.* Oxford.

ELIAS, M., P. COTTE 2008. Multispectral camera and radiative transfer equation used to depict Leonardo's sfumato in Mona Lisa. *Applied Optics* 47(12), 2146–2154.

EVERITT, B.S., S. LANDAU, M. LEESE 2011. *Cluster Analysis*, 5th edition. New York.

HALL, E.T., F. SCHWEIZER, P.A. TOLLER 1973. X-Ray Fluorescence analysis of museum objects: A new instrument. *Archaeometry* 15(1), 53–78.

JAVANSHAH Z. 2018. Chemical and mineralogical analysis for provenancing of the Bronze Age pottery from Shahr-i-Sokhta, south eastern Iran. *Scientific Culture* 4(1), 83–92.

KOLONIA, R., S. TSAROUCHAS 2001-2004. *Archaiologikon Deltion* 56-59, 424 (in Greek).

KUNICKI-GOLDFINGER, J., J. KIERZEK, A. KASPRZAK, B. MAŁOZEWSKA-BUĆKO 2000. A study of eighteenth century glass vessels from central Europe by X-ray fluorescence analysis. *X-Ray Spectrometry* 29, 310–316.

LANGHOFF, N., V.A. ARKADIEV, A.A. BJEOUMIKHOV, H.E. GORNY, J. SCHMALZ, R. WEDELL 1999. Concepts for a portable X-ray spectrometer for non-destructive analysis of works of art. *Berliner Beiträge zur Archäometrie* 16, 155–161.

LIRITZIS, I., E. POLYCHRONIADOU 2007. Archaeometrical analysis of mural paintings made by Spyros Papaloukas (1892–1957) in Amfissa cathedral. *ARCHEOSCIENCES, Revue d'Archéométrie* 31, 1–16.

LIRITZIS, I., N. ZACHARIAS 2010. Portable XRF of archaeological artifacts: current research, potentials and limitations. In: M.S. Shackley (ed.), *X-ray Fluorescence Spectrometry (XRF) in Geoarchaeology*, 109–142. New York.

LONGONI, A., C. FIORINI, P. LEUTENEGGER, S. SCIUTI, G. FRONTEROTTA, L. STRÜDER, P. LECHNER 1998. A portable XRF spectrometer for non-destructive analyses in Archaeometry. *Nuclear instruments and*

methods in Physics research Section A: Accelerators, spectrometers, detectors and associated equipment 409(1-3), 407–409.

MOROPOULOU, A., N. ZACHARIAS, E.T. DELEGOU, B. MARÓTI, Z. KASZTOVSZKY 2016. Analytical and technological examination of glass tesserae from Hagia Sophia. *Microchemical Journal* 126, 170–184.

NÖLLER, R. 2015. Cinnabar reviewed: characterization of the red pigment and its reactions. *Studies in Conservation* 60 (2), 79–87.

OIKONOMOU, A., K. BELTSIOS, N. ZACHARIAS, V. ARAVANTINOS, P. TRIANTAFILLIDIS 2012. Ancient glass from mainland Greece and the Aegean. In: N. Zacharias, M. Georgakopoulou, K. Polikreti, G. Fakorellis, and Th. Vakoulis (eds) *Proceedings of the 5th Synposium of the Hellenic Society for Archaeometry*, 507–527. Athens (in Greek).

OIKONOMOU, A., J. HENDERSON, M. GNADE, S. CHENERY, N. ZACHARIAS. 2016. An archaeometric study of Hellenistic glass vessels: evidence for multiple sources. *Archaeological and Anthropological Sciences* 10(1), 97–110.

PALAMARA, E., N. ZACHARIAS, L. PAPAKOSTA, D. PALLES, E.I. KAMITSOS, J. PIREZ-ARANTEGUI 2016. Studying a funerary Roman vessel glass collection from Patras, Greece: An interdisciplinary characterisation and use study. *STAR: Science & Technology of Archaeological Research* 2, 1–14.

PAPADOPOULOU, D., A. SAKALIS, N. MEROUSIS, N.C. TSIRLIGANIS 2007. Study of decorated archaeological ceramics by micro X-ray fluorescence sprctroscopy. *Nuclear Instruments and Methods in Physics Research Section A: Accelerators, Spectrometers, Detectors and Associated Equipment* 580(1), 743–746.

PAPAGEORGIOU, I., I. LIRITZIS 2007. Multivariate mixture of normals with unknown number of components: An application to cluster Neolithic ceramics from Aegean and Asia Minor using portable XRF. *Archaeometry* 49(4), 795–813.

PARIENTE, A. 1991. *Les céramiques, Guide de Delphes-Le Musée*. Paris.

PERDRIZET, P. 1908. Monuments figurés, petits bronzes, terre-cuites, antiquités diverses. *Fouilles de Delphes* V, 165. Paris.

READE, W.J., K.L. PRIVAT 2016. Chemical characterisation of archaeological glasses from the Hellenistic site of Jebel Khalid, Syria by electron probe microanalysis. *Heritage Science* 4, 20.

SHORTLAND, A.J., H. SCHROEDER 2009. Analysis of first millenium BC glass vessels and beads from the Pichvnari necropolis, Georgia. *Archaeometry* 51(6), 947–965.

SOKARAS, D., A.G. KARYDAS, A. OIKONOMOU, N. ZACHARIAS, K. BELTSIOS, V. KANTARELOU 2009. Combined elemental analysis of ancient glass beads by means of ion beam, portable XRF, and EPMA techniques. *Analytical and Bioanalytical Chemistry* 395(7), 2199–2209.

SPOTO, G., A. TORRISI, A. CONTINO 2000. Probing archaeological and artistic solid materials by spatially resolved analytical techniques. *Chemical Society Reviews* 29, 429–439.

VANDENABEELE, P., L. MOENS 2000a. Micro-Raman spectroscopy applied to the investigation of art objects. In: *Proceedings SPIE 4098, Optical Devices and Diagnostics in Materials Science*, 232–240. Bellingham.

VANDENABEELE, P., B. WEHLING, L. MOENS, H. EDWARDS, M. DE REU, G. VAN HOOYDONK 2000b. Analysis with micro-Raman spectroscopy of natural organic binding media and varnishes used in art. *Analytica Chimica Acta* 407(1-2), 261–274.

WOBRAUSCHEK, P., G. HALMETSCHLAGER, S. ZAMINI, C. JOKUBONIS, G. TRNKA, M. KARWOWSKI 2000. Energy-dispersive X-ray fluorescence analysis of Celtic glasses. *X-Ray Spectrometry* 29(1), 25–33.

WU, J., P.L. LEUNG, J.Z. LI, M.J. STOKES, T.W. MIKE 2000. EDXRF studies on blue and white Chinese Jingdezhen porcelain samples from the Yuan, Ming and Qing dynasties. *X-Ray Spectrometry* 29(3), 239–244.

ZACHARIAS, N., K. BELTSIOS, A. OIKONOMOU, A.G. KARYDAS, Y. BASSIAKOS, C.T. MICHAEL, C. ZARKADAS 2008. Solid-state luminescence for the optical examination of archaeological glass beads. *Optical Materials* 30, 1127–1133.

ZACHARIAS, N., Y. BASSIAKOS, B. HAYDEN, K. THEODORAKOPOULOU, T.M. CHRISTODOULOS 2009. Luminescence dating of deltaic deposits from eastern Crete, Greece: Geoarchaeological implications. *Geomorphology* 109(1-2), 46–53.

ZACHARIAS, N., M. KAPAROU, G. MASTROTHEODOROS, A.R. OIKONOMOU, K. BELTSIOS, T. TSELIOS, V. ARAVANTINOS, K. KALIGA, D. OIKONOMOU 2012. Technological study of pyrometallurgical products of the excavation site dedicated to the worship of Hercules, near Electrai Pylai (Kadmia), Thebes. In: N. Zacharias, M. Georgakopoulou, K. Polikreti, G. Fakorellis, and Th. Vakoulis (eds), *Proccedings of the 5th Symposium of the Hellenic Society for Archaeometry*, 345–364. Athens (in Greek).

Appendix A. The groups represented in Figure 7 and their consistent samples

Group 1		Group 2		Group 3	Group 4
MAN01	Sa.22	2-Py945/T25a	JK25	JK03	JK26
MAN02	Sa.23	4-Py133	JK29	JK18	JK46
MAN03	Sa.32	6-Py3543	JK32	JK24b	Sa.2
MAN04	Sa.43	10-Py519/521b	JK33	JK31	Sa.3
MAN05	SAT.3	14-Py6267a	JK34	JK38b	Sa.7
MAN06	SAT.6	21-Py6435	JK35	JK42	Sa.8
MAN07	SAT.7	22-Py6436	JK38a	JK50	Sa.9
MAN08	SAT.8	27-Py8372	JK39	Sa.25	Sa.10
1672	SAT.9	28-Py8372	JK40	Sa.29	Sa.11
1673	SAT.11	39-Py872	JK41	Sa.30	Sa.12
1674	Pic16b	54-Mth1309	JK43	Sa.41	Sa.13
5-Py3543B	Pic21b	62-Mth824	JK44	Sa.42	Sa.14
7-Py369b	Pic37	JK01	JK45	Sa.44	Sa.15
15-Py6273	R.8	JK02	JK47	Pic30b	Sa.18
18-Py6299	R.11	JK04	JK48	Pic27b	Sa.20
29-Py8382	R.15	JK05	JK49	Pic40	Sa.24
37-Py8483	R.23	JK06	JK51	Pic41	Sa.26
55-Mth2898	R.29	JK07	JK53	Pic47a	Sa.27
60-Mth338	R.33	JK08	JK54	Pic47c	Sa.31
61-Mth822	R.53	JK09	JK55	T.3	Sa.33
JK28	R.69	JK10	JK56	T.4	Sa.34
JK30	T.1	JK11	JK57	T.5	Sa.36
Sa.4	T.2	JK12	JK58	T.11	Sa.37
Sa.5	T.6	JK13	JK60	T.12	Sa.38
Sa.16	T.9	JK14	Sa.28	T.13	Sa.39
Sa.21	T.19	JK15	SAT.10	T.17	SAT.2
Sa.35	T.21	JK16	Pic21a	T.18	Pic16a

Sa.40	T.23	JK19	Pic28c	T.20	Tsi4b
SAT.5	T.25	JK21	Tsi4a	T.22	Pic46a
Sa.1	T.26	JK22	Pic46b	T.24	T.10
Sa.6	T.27	JK23	Pic47b	T.28	
Sa.17	T.29	JK24a			
Sa.19					